TRANSVERSE BEAM PROFILE DIAGNOSTIC USING FIBER OPTIC ARRAY*

S. Wu#, G. Andonian, T. Campese, A. Murokh, R. Agustsson,
RadiaBeam Technologies, Santa Monica, CA 90404, USA
R.K. Li, UCLA, Los Angeles, CA 90095, USA
M. Fedurin, R. Malone, K. Kusche, C. Swinson,
Brookhaven National Laboratory, NY 11961, USA

Abstract

The fiber-mesh diagnostic (FMD) is a transverse beam profile diagnostic based on the emission and detection of Cherenkov radiation produced as a relativistic electron beam traverses through an ordered bundle of fiber optics (SiO_2), arranged in a hexagonal close-pack configuration. Sub-10μm transverse beam profile resolution is attainable due to fiber optic core concentricity. Adequate SNR is achieved using a standard CCD sensor. A fiber optic taper input maximizes light collection efficiency by coupling each output channel to approximately single-pixel pitch. A v-groove holder and assembly process was developed to hold many fiber layers in the desired configuration. In this paper, we present results from a fully functional FMD prototype evaluated at the BNL ATF facility that demonstrates the efficacy of this diagnostic.

INTRODUCTION

The FMD was developed to address the need for higher resolution transverse profiling in low emittance electron beams. Standard techniques to measure the transverse extent of beams include fluorescent screens (such as YAG), observation of optical transition radiation, wire scanners and others. The resolution limit of these diagnostics hovers around >20μm. In the FMD, Cherenkov radiation is generated when a charged particle strikes a dielectric fiber that is placed at the Cherenkov angle. The device collects incoherent Cherenkov radiation, so the spatial profile is an accurate representation of the beam transverse charge distribution.

For a relativistic beam striking a dielectric, the Cherenkov angle, θ_C, is:

$$\theta_C = \cos^{-1}\frac{1}{n} \cong 46.5° \qquad (1)$$

where n is refractive index of the fiber.

The approximate photons generated in each fiber are:

$$N_{photons} \approx \frac{2\alpha}{\sqrt{\pi}} N_e \left[\frac{d^2}{\lambda\sigma_x}\right]\left(\frac{\Delta\omega}{\omega}\right) NA \qquad (2)$$

where α is the fine structure constant, d is the fiber core diameter, λ is the wavelength of light, N_e is the number of electrons, σ_x is electron beam RMS width, and $\Delta\omega/\omega$ is the fiber bandwidth.

A proof-of-concept experiment was executed at the UCLA Pegasus lab to demonstrate adequate photon yield for a single fiber [1]. The experiment results and theory were scaled for Brookhaven ATF parameters (Table 1). These results proved the feasibility to build a functioning prototype.

Table 1: Electron Beam Test Parameters

Facility	Energy (MeV)	Charge (pC)	Expected Photon Yield
UCLA Pegasus	2.5	25	10^4
Brookhaven ATF	57.6	100-1000	10^5-10^6

SYSTEM DESCRIPTION

The interaction point consists of an ordered array of single mode fiber optics (Fluorine-doped SiO_2, 6.8μm MFD, 245μm OD), which are also used at CERN for their radiation resistant qualities [2], to obtain multiple measurements in one instance. Cherenkov radiation is generated within the fibers, which also guide the radiation to an external CCD detector. Custom algorithms convert the multiple-fiber signals to a transverse profile charge distribution on a shot-to-shot basis.

The system consists of three key components:

(1) The fiber array at the interaction point
(2) The CCD acquires the Cherenkov signal
(3) DAQ logic converts signals to beam profile

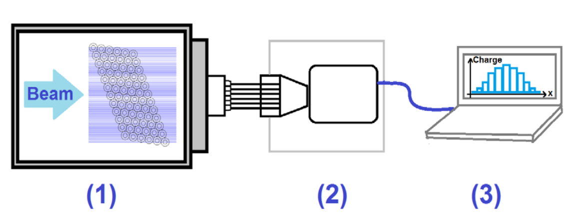

Figure 1: Diagram of System Design.

*Work is supported by U.S. D.O.E. Contract Number DE-SC0000870
#swu@radiabeam.com

ISBN 978-3-95450-138-0

Fiber Holder Fabrication and Assembly

The fibers are bundled in a hexagonal configuration so that each core position is set. They are held together with a v-groove clamping method:

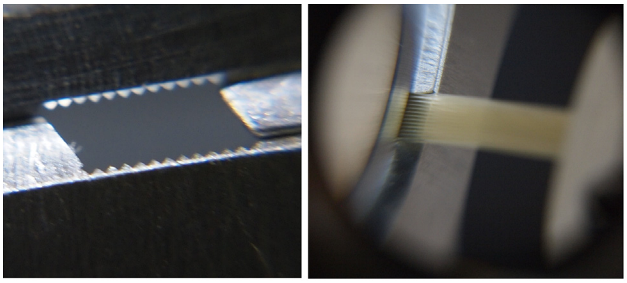

Figure 2: Photograph of fiber array. Fibers are clamped with v-grooves (Left). Fibers Assembled to holder (Right).

In order to correctly arrange fibers to the holder, fibers are initially bundled to single rows of 12. The first row settles into the v-grooves, and remaining bundles are laid onto the grooves of the previous layer. The tooling holds each layer taut during this process:

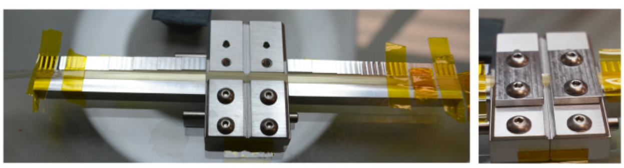

Figure 3: Tooling for holder assembly.

After the fibers are clamped to the holder, the holder arms are pulled apart, and fastened to the insertion rod:

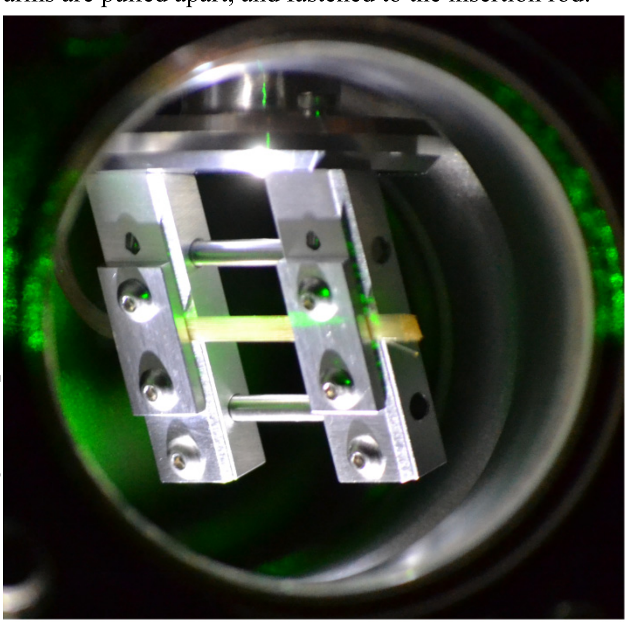

Figure 4: Fiber holder assembly in situ.

Camera Design

To maximize light collection efficiency, the fiber ends are mounted to a fiber optic taper input bonded directly to the CCD, providing a robust mounting surface. The result is focused light achieving almost single-pixel coupling, which optimizes the system's detection limit.

12-bit digital output is sent to the computer via Ethernet, enabling long distance data transmission needed from the experimental hall to the control room.

Data Acquisition

Prior to operation, fiber positions on the camera input are located by illuminating the fibers pointing to the camera. The sum of a 5x5 pixel region-of-interest for each location is ordered so that it represents the transverse position of each fiber core.

MATLAB interfaces with the camera. A TTL signal triggers the camera to capture an image, which is real-time processed to display the updated transverse profile. Background is subtracted from the profile, and the mean and RMS are calculated (See Fig. 5).

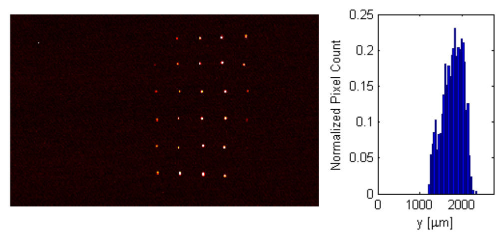

Figure 5: Raw image (Left), Single shot profile (Right).

RESULTS

The experiment was executed at Brookhaven ATF. YAG screens located on both sides of the FMD were used to benchmark the device under test.

Beam Width Measurements

YAG-based profile monitors along the beamline were used to tune the beam and for comparative studies with the FMD. A parabolic fit to the YAG-profile measurements was applied to calculate the expected beam width at the FMD location. Three beam widths were measured at 500pC and compared to the FMD measurements. The results are displayed in Figure 6, and shown in Table 2.

Table 2: Beam Width Comparisons at FMD Location

Calculated Width [µm] (YAG-profile monitors)	**Measured Width [µm] (FMD)**
171	139
341	365
448	449

ISBN 978-3-95450-138-0

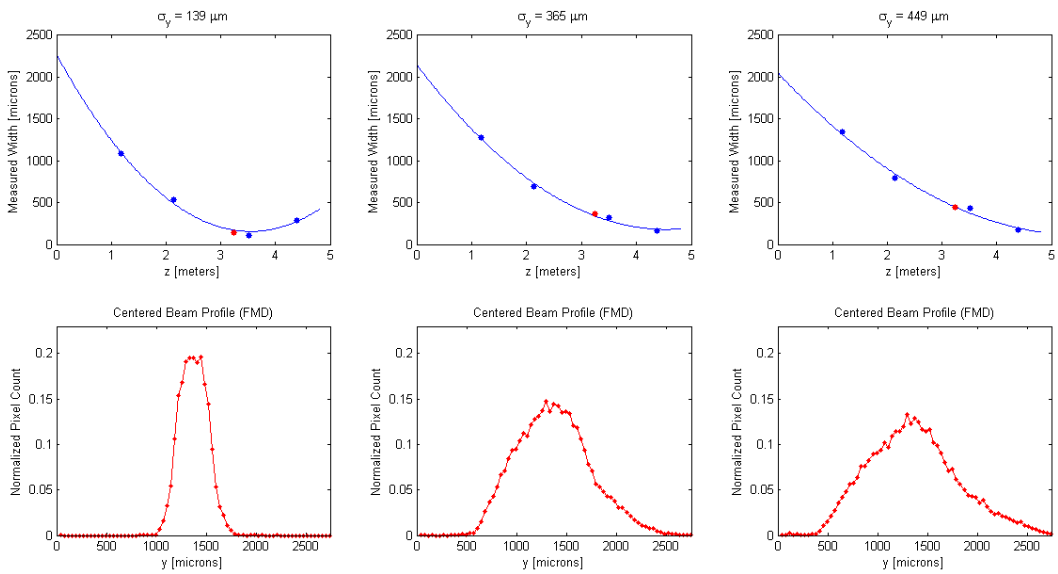

Figure 6: Top Row –Beam widths measured with YAG screens along the beamline (blue). Beam width measured with FMD plotted at the measured z- distance (red). Bottom Row – The averaged beam profile as measured with FMD.

The beam was also intentionally detuned to record a "non-Gaussian" profile with the FMD at 500pC (See Fig. 7) to observe profile features on the ~10μm scale.

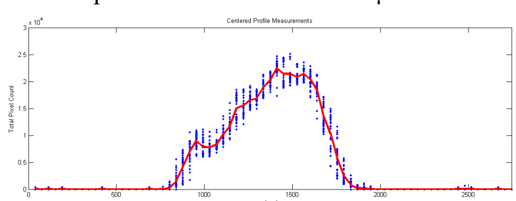

Figure 7: Each shot is centered (blue), and the averaged profile is calculated (red).

Quadrupole Scans

The current in an upstream quadrupole magnet was varied and the beam widths were recorded with FMD and a YAG-based profile monitor. The beam charge was 80pC. The emittance is calculated for both diagnostics and shows reasonable agreement (see Table 2).

Table 2: Comparison of Calculated Emittance

Diagnostic	Quad Distance [meters]	ϵ_n [mm-mrad]
YAG	2.58	4.2E-06
FMD	2.32	3.9E-06

CONCLUSION

The Fiber Mesh Diagnostic uses beam-generated Cherenkov radiation within a fiber optic array to characterize the beam transverse profile. The prototype was tested at the BNL ATF and its accuracy was compared to the YAG-profile monitors. The results were successful and demonstrated the viability of this diagnostic for high-precision transverse beam profile characterization. Future tests will address issues of fiber lifetime in high-radiation environments and an upgraded user-interface.

ACKNOWLEDGMENT

The authors would like to thank the staff at UCLA Pegasus and Brookhaven National labs for their expertise and the operation of their facilities. Work supported by DOE SBIR Grant No. DE- SC0000870.

REFERENCES

[1] R. Tikhoplav *et al.*, "Progress Report on Development of a High Resolution Transverse Diagnostic Based on Fiber Optics", *Proceed. IPAC 12,* MOPPRO090 (2012); http://www.JACoW.org
[2] "Fiber resists CERN's radiation to carry data," Newsdesk, May 2007, Historical Archive; http://www.optics.org/article/27855

ISBN 978-3-95450-138-0